Research and analysis of elastic strip fatigue under stress controlled loading mode

J Huang, Z Wu*, X Y Zhang
Faculty of Civil Engineering and Architecture, Kunming University of Science and Technology, Kunming, 650504, China

ABSTRACT
Fastener technology is a key technology of Ballastless track structure in high-speed railway, and the elastic strip is the key component to realize fastener function. To this end, a special loading fixture is fabricated to explore the performance of the elastic strip under fatigue load. The working state of the elastic strip was simulated through the fatigue testing machine, and the stress-controlled loading modes and four loading amplitudes (25±5kN, 25±7.5kN, 25±10kN, 25±12.5kN) are investigated. The pressure control method is used for fatigue tests, and the results show that: (1) As the load amplitude increases, the fatigue life decreases sharply and its decreasing speed is greater than the increasing speed of load amplitude; (2) The buckling pressure and displacement curves of the elastic strip have the characteristics of "increasing step-by-step" and "decreasing step-by-step"; (3) In the fatigue test, the attenuation of buckling pressure is 22% - 33% and the displacement at the front end of the ring is 18% - 25%; (4) According to the results, the buckling pressure curve and the displacement curve of the ring in the elastic strip are drawn, and the equations of them are fitted to estimate the service performance of the elastic strip.

1. INTRODUCTION

Fastener technology is a key technology of Ballastless track, and the elastic strip is one of the key components of the fastener system that is most prone to fatigue damage. The designed fatigue life of an elastic strip is generally between 3 million and 5 million times with high cycle fatigue and small deformation [1-4]. In practical engineering, the service life of the elastic strip is often lower than the designed fatigue life. This causes a large number of elastic strips on the line to break in advance, resulting in insufficient lateral buckling pressure and longitudinal resistance of the track, seriously threatening the safety of trains [5-8]. In addition, according to the standard of laying two groups of elastic strips every 62.5 cm on the Ballastless track, i.e., four elastic strips are laid at each transverse node, an average of 160,000 elastic strips need to be laid on a track every 100 kilometers. The elastic strips need to be laid on two-way or even multi-track sections. In practice, too many elastic strips will lead to the failure of fastener and endanger driving safety [9-13]. The maintenance workload and cost of replacing new bomb strips along the railway are increasing [14-17]. As such, studying the fatigue of elastic strips becomes more important. However, conventional fatigue tests cannot accurately simulate the actual working state of elastic strips and is easy to cause a large difference between the test results and the actual situation. In the fatigue test, a special mold was made to accurately simulate the actual working state of the elastic strips [18-20]. Through the fatigue tests of WJ-7 under different loadings, the change of buckling pressure and ring displacement

*Corresponding Author: qfwuedu@sina.com

with cycles N was comparatively studied to analyze the fatigue characteristics [21-22]. Fasteners are the key components that connect the rail and the under-rail structures, and also the components with the most severe fatigue wear in the track structure [23]. The fatigue test and analysis of the elastic strip under different working conditions have good theoretical and practical significance.

2. PRINCIPLE, ASSEMBLY AND PROCEDURE OF FATIGUE TEST

2.1. Principle of fatigue test

The fatigue test of metal materials usually adopts constant amplitude loading, i.e., cyclic loading between the maximum stress value_$\sigma_{\max}$ and the minimum stress value_$\sigma_{\min}$ [24-27]. The difference between_$\sigma_{\max}$ and_$\sigma_{\min}$ is the stress range, i.e., $\Delta\sigma$, and the stress amplitude_a is one half of $\Delta\sigma$ in the stress range. The mean value of sigma $\sigma_{\max}$ and sigma $\sigma_{\min}$ is the average stress value m. There are also two commonly used parameters, as shown in Eq. (1):

$$\begin{cases} R = \frac{\sigma_{\min}}{\sigma_{\max}} \\ A = \frac{\sigma_a}{\sigma_m} \end{cases} \tag{1}$$

where R is the stress ratio and A is the amplitude ratio.

Under a certain R, when the material component is subjected to the maximum stress_$\sigma_{\max}$, failure or fracture would occur after N stress cycles, and then N is the fatigue life of the component under the maximum stress_$\sigma_{\max}$. The previous experiments found that the higher the cyclic stress, the shorter the component life, the lower the cyclic stress, the longer the component life. In this way, a stress life curve can be drawn from the experimental data, that is, the S-N curve of the component material [28-31], as shown in Fig. 1.

It can be seen from the Fig. 1 that under a certain R, when the stress amplitude S is less than a certain limit, the fatigue life N of the material tends to be infinite, that is, the material will not suffer fatigue damage. The corresponding stress amplitude S is called the endurance limit or the fatigue limit of the material. The cyclic radix N0 is approximately equal to the fatigue life of an infinite material when the component has not been destroyed by N0 cycles, and the experiment cannot be carried out permanently [32-35]. Generally, N0 of the steel and concrete is taken as 107 and 106, respectively.

The above analysis is based on the stress of material fatigue, and this chapter would focus on the variation law of toe buckling pressure and the ring displacement of the elastic strip. The longitudinal axis of the curve is replaced by the stress amplitude S with the buckling pressure P at the left and right toes of the elastic strip and the displacement X of the ring of the elastic strip. Accordingly, the S-N curve of the elastic strip is changed into the P-N curve and X-N curve.

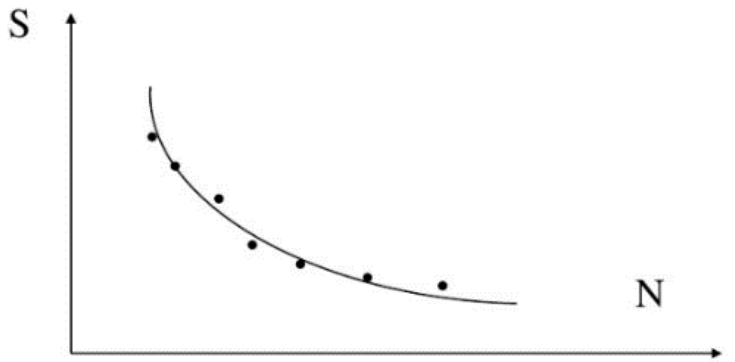

Fig.1. S-N curve of material

2.2. Fatigue test assembly

Type WJ-7 elastic strip fatigue testing machine adopts this system, which can be used for high and low cycle fatigue, crack growth rate, tensile compression bending, fracture toughness KIC, fracture toughness JIC and component life simulation test. The main technical indicators are maximum 100kN test force, ±75mm travel time and maximum 75Hz load frequency, as shown in Fig. 2. MTS in Fig. 2 can be used for fatigue test.

Fig. 2. MTS810 servo hydraulic test system

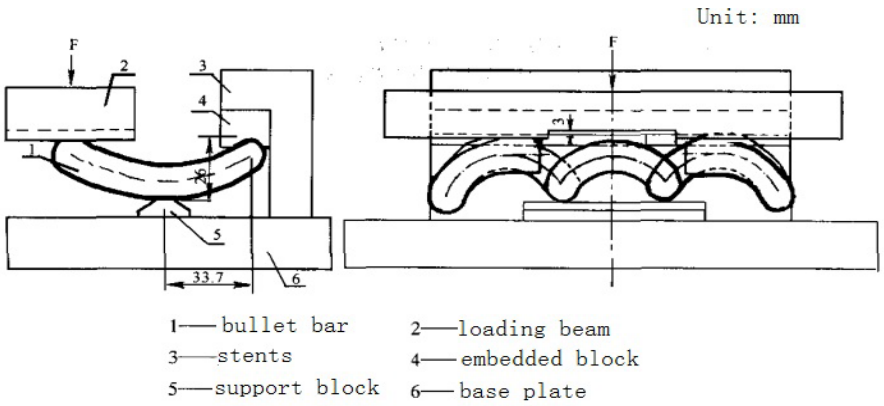

(a)

(b)

Fig. 3. Schematic diagram of fatigue test device for type I and II elastic strips

The general fatigue test method for elastic strips in China is the "Fatigue Test Method for Elastic Strip Type I and Type II Fasteners" issued by the Railway Corporation (formerly the Ministry of Railways) in 2002, mainly referring to the German standard DB-TL918 127. The test device is shown in Fig. 3. The method is to measure the initial relative height of the mid-circle of the elastic strip before the test, and then apply the dynamic displacement to the loaded beam. After 106 load cycles, the relative height of the mid-circle is measured, i.e., the residual deformation_Δh of the elastic strip is obtained. This test method can directly obtain the ring displacement of the elastic strip after N cycles but cannot obtain the buckling pressure change caused by fatigue wear and the ring displacement and strain of the elastic strip before failure.

A special die suitable for MTS810 system is made in the fatigue test to measure the buckling pressure of the left and right toes and the displacement of the ring in real-time. The mold design is shown in Fig. 4(a)-(c), and the mold is shown in Fig. 4 (d). Each part of the mold is removable and can be replaced when some parts are worn or even destroyed in the experiment. In order to accurately simulate the real contact situation, the large arc back-end support of the elastic strip on the mold is taken from the iron pad of the original WJ-7 fastener system.

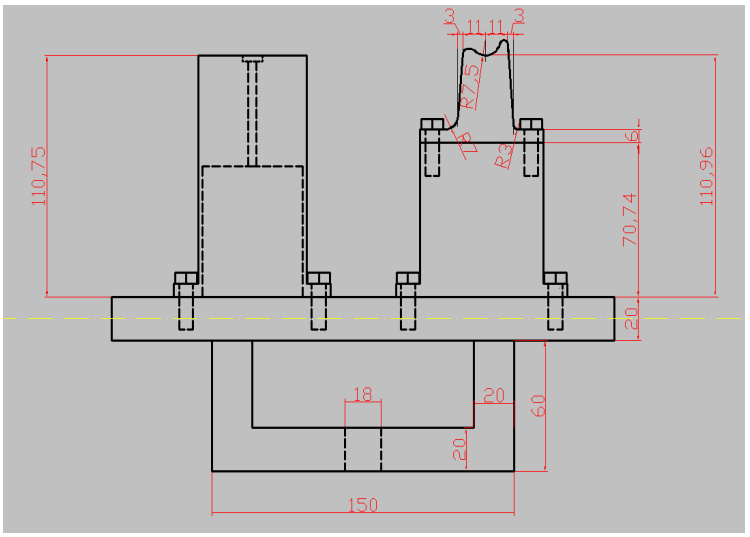

(a) Left view of die (unit: mm)

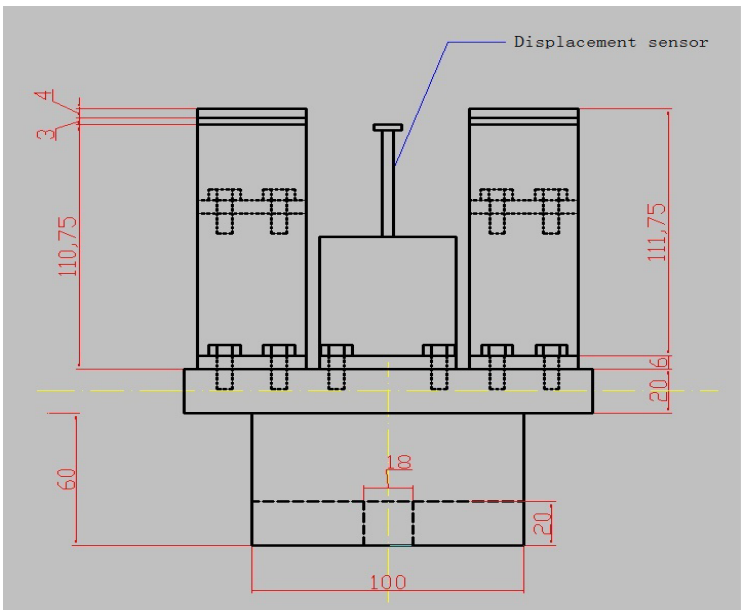

(b) Front view of die (unit: mm)

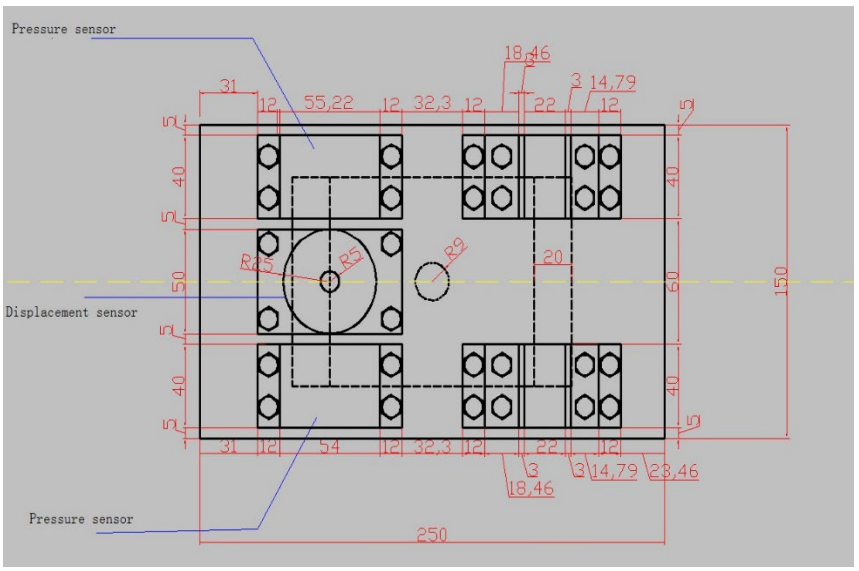

(c) Top view of die (unit: mm)

(d) Solid mold

Fig.4. Solid drawing and design drawing of support

CFBLZ pressure sensors are installed on the left and right sides of the mold (as shown in Fig. 5), and D020 strain displacement sensors are installed in the middle (as shown in Fig. 6).

Fig.5. CFBLZ pressure sensor

Fig.6. D020 displacement sensor

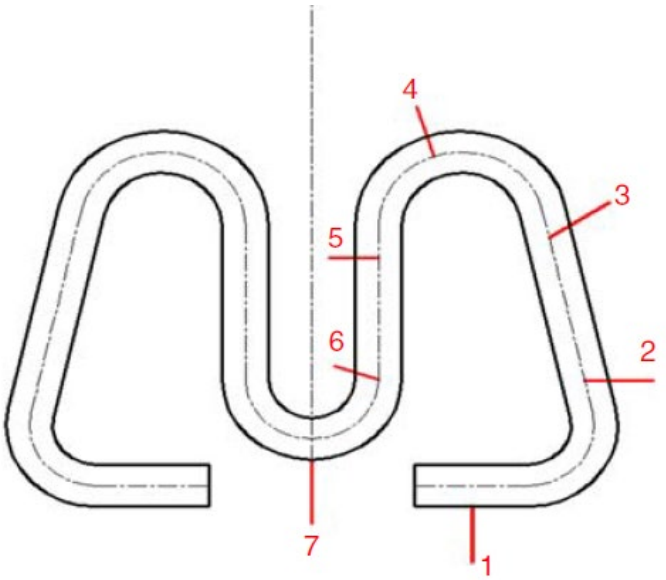

(a) Measuring position in elastic strip

(b) Assembly test drawing

Fig.7. Fixture assembly diagram of elastic strip fatigue test

As shown in Fig. 7, the wire rings on the left and right sides of the assembly are protective to prevent the broken limb from flying out after the elastic strip is fatigued and fractured, and its influence on the stress of the elastic strip and the test results can be neglected. The pressure sensor and displacement sensor are connected to the DH15202 controller of the MTS810 test system to control the pressure and displacement loads based on the readings of the two sensors.

2.3. Fatigue test procedure

Before the fatigue test, it is necessary to determine and set various parameters, such as the applied load waveform, the applied load frequency, the upper and lower limits of the pressure load control mode, the upper and lower limits of the loading model controlled by the displacement, the pressure and displacement data acquisition interval, so as to set the maximum upper limit of the protective pressure and the displacement for instruments, data acquisition and channel.

According to the test cost and time, the range of increase and decrease is 2.5kN and the load frequency is 5Hz. In the fatigue test, the sinusoidal wave load is adopted. According to relevant provisions of the Technical Instructions for All Kinds of Fasteners, the corresponding bolt buckling pressure of WJ-7 elastic strip under normal installation is 25 kN. In this fatigue test, under the pressure-controlled loading mode, the pressure load of 25 kN is considered as the equilibrium position and the displacement is correspondingly considered as the displacement in the pressure-controlled loading mode. In the load-controlled mode, the value of 25kN displacement ring corresponds to the equilibrium position. The preliminary tests of WJ-7 elastic strip showed that under a fatigue load of 25±3 kN, the number of elastic strip fractures did not exceed 5 million times and the buckling pressure of the front toe and the displacement of the ring did not change significantly. The load cycles are much greater than the basic number of 107 cycles for steel. Compared with the actual working conditions, the fatigue loads are set to 25±5 kN, 25±7.5 kN, 25±10 kN and 25±12.5 kN, respectively.

On the one hand, if the load frequency is set too fast, the instrumentation may be unstable because of the system stiffness of MTS810. On the other hand, the actual applied load lags behind the measurement feedback of the pressure sensor and displacement sensor, resulting in inaccurate experimental results. If the frequency is set too slow, WJ-7 elastic strip is subject to high cycle fatigue test at small deformations. A single life cycle is time-consuming and inefficient, requiring a lot of human and material resources. After comprehensive comparison, the load frequency is finally set to 5Hz.

The interval should not be too small in data acquisition, because too large data file will bring trouble for subsequent data screening and processing. The interval also should not be too large, especially in the late fatigue test; too large interval will result in critical data being acquired in the pre-fracture stage. In the early stage of the experiment, the acquisition interval is set to 500 times, that is, a complete sinusoidal waveform is collected every 500 times. In the late stage of the experiment, the acquisition interval is set to 200 times, and the sampling frequency is set to 0.2 seconds. The channels of data acquisition mainly include Ch1 Displacement (instrument displacement), Ch1 Force (instrument load), Input 1 (displacement sensor), Input 2 (left front toe pressure sensor), and Input 3 (right front toe pressure sensor).

Before the experiment, the specimens need to be preloaded, which is generally 0.3-0.4 times of the ultimate load, and 10 kN is applied in this test. During the loading, the data of Input 1 channel are observed to judge whether the middle ring of the elastic strip is in good contact with the sensor, whether the geometric center of the elastic strip is aligned with the loading system and whether the elastic strip is in an axial stress state. After all indications are normal, they are slowly unloaded to 0.1-0.5 kN.

3. FATIGUE RESULTS AND ANALYSIS

3.1. Fatigue test under pressure loading controlled loading mode

WJ-7 elastic strip was subjected to constant amplitude cyclic loading. The pressure amplitudes are 25±5 kN, 25±7.5 kN, 25±10 kN and 25±12.5 kN, respectively, and three elastic strip specimens were tested. Due to the large amount of fatigue test data and200 data points under the same cycle count, it is necessary to screen out some similar data. The cyclic load is based on 25 kN, and 25 kN is also the buckling pressure when the elastic strip is normally installed. Ch1 Force is set to about 25 kN (24.95kN-25.05 kN) corresponding to other channels of numerical screening for comparison. The most typical flexion pressure of the left and right front toes and the displacement data of the mid-circle of the elastic strip were selected to analyze three samples under the same pressure amplitude [35]. Fatigue test loads cover the possible load range under actual working conditions and are close to the actual situation.

3.2. Fatigue test results and analysis of pressure-controlled loading mode under the cyclic loading of 25± 12.5kN

During the processing cycle, the measurement data of 25±12.5 kN under cyclic loading were collected 1000 times. The measurement data of the front end displacement and the pressure of the left and right ends of the elastic strip are shown in Table 1(The first column of the last row is fatigue life.).

Table 1. Measurement data of elastic parts under 25±12.5kN cyclic loading

Cycle count of Ch1	Aux Input1 (displacement of the front end of the stripe) /mm	Aux Input 2 (pressure on the left side of the elastic strip)/kN	Aux Input 3 (pressure on the right side of the elastic strip)/kN	Total pressure deduction /kN
500	16.077	5.174	5.427	10.601
1500	16.222	5.128	5.370	10.498
2500	16.453	5.042	5.298	10.340
3500	16.574	4.976	5.210	10.186
4500	16.675	4.935	5.177	10.112
5500	16.751	4.919	5.160	10.079
6500	16.798	4.902	5.148	10.050
7500	16.945	4.834	5.065	9.899
8500	17.078	4.777	5.007	9.784
9500	17.171	4.742	4.942	9.684
10500	17.234	4.731	4.907	9.638

Table 1 (cont.). Measurement data of elastic parts under 25±12.5kN cyclic loading

Cycle count of Ch1	Aux Input1 (displacement of the front end of the stripe) /mm	Aux Input 2 (pressure on the left side of the elastic strip)/kN	Aux Input 3 (pressure on the right side of the elastic strip)/kN	Total pressure deduction /kN
11500	17.309	4.646	4.885	9.531
12500	17.483	4.581	4.831	9.412
13500	17.607	4.546	4.796	9.342
14500	17.681	4.528	4.778	9.306
15500	17.712	4.518	4.768	9.286
16500	17.763	4.510	4.760	9.270
17500	17.819	4.506	4.756	9.262
18500	17.885	4.501	4.751	9.252
19500	17.931	4.482	4.732	9.214
20500	17.957	4.463	4.713	9.176
21500	17.993	4.454	4.704	9.158
22500	18.039	4.425	4.675	9.100
23500	18.065	4.412	4.662	9.074
24500	18.084	4.403	4.648	9.051
25500	18.152	4.398	4.621	9.019
26500	18.201	4.352	4.583	8.935
27500	18.234	4.309	4.559	8.868
28500	18.321	4.291	4.541	8.832
29500	18.378	4.284	4.523	8.807
30500	18.435	4.270	4.499	8.769
31500	18.472	4.251	4.474	8.725
32500	18.518	4.238	4.460	8.698
33500	18.554	4.232	4.453	8.685
34500	18.711	4.208	4.428	8.636
35500	18.792	4.116	4.356	8.472
36500	18.853	4.045	4.295	8.340
37500	18.894	3.998	4.248	8.246
38500	18.924	3.966	4.216	8.182
39500	18.944	3.942	4.192	8.134

As shown in Table 1, the buckling pressure and ring displacement curves of the elastic strip under cyclic loading are shown in Fig. 8.

As shown in Fig. 8, the buckling pressure and the ring displacement of the elastic strip change greatly in the initial stage, which is small in the middle stage and has a big turning point in the final stage. At the same time, the buckling pressure and displacement curves of the elastic strip have the characteristics of "step increasing" and "step decreasing". This is because that the plastic deformation of the elastic strip under cyclic loading is periodic. In the

case of large plastic deformation, the buckling pressure and displacement change fast without plastic deformation or plastic deformation. The smaller the stage, the smaller the buckling pressure. The buckling pressure of the strip lost a lot at the beginning of the test, and the size was 10.6kN. The buckling pressure decreases little due to a short fatigue life of the elastic strip under loading, and it decreased to 8.1kN at the end of the test. It is stipulated in the Technical Instructions for All Kinds of Fasteners that the buckling pressure of a single WJ-7 elastic strip should not be less than 9 kN, and that of the elastic strip at the end of the test should be less than this minimum value. At the beginning of the test, the center circle displacement of the elastic strip increased from 13 mm to 16 mm. When the loading pressure was 35kN, the elastic strip would have plastic deformation and buckling pressure loss. The plastic deformation increased further when the cyclic load was 37.5 kN. The equilibrium position of 25 kN was at the beginning of the test, and the center shift of the strip increased to about 16mm. At the end of the test, the displacement of the ring in the elastic strip changed from 16mm to about 19mm, which was close to the limit value of the elastic range.

(a)

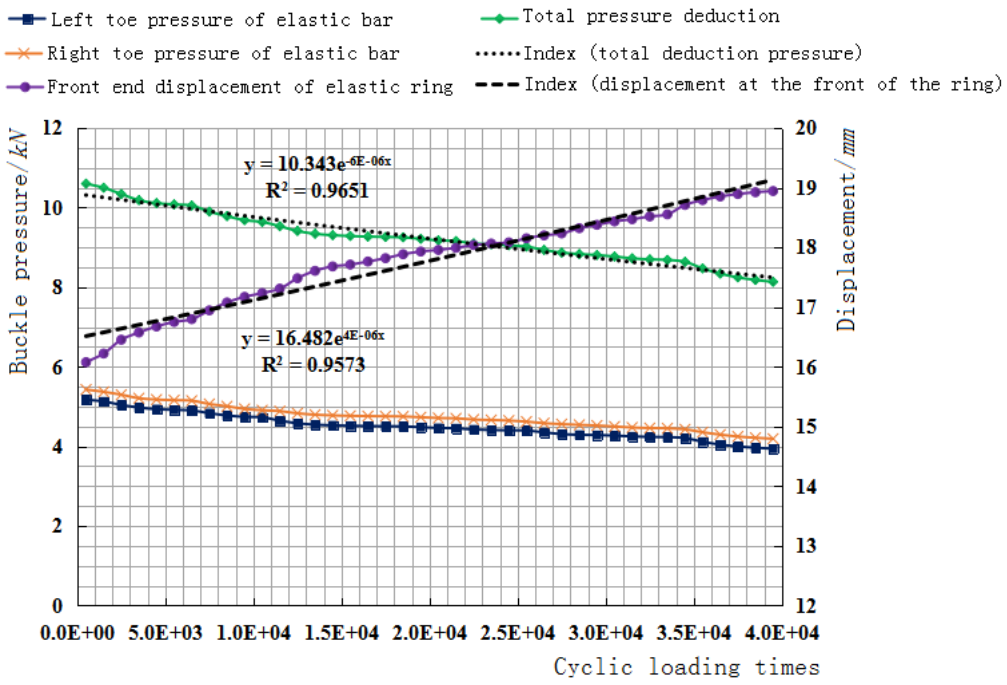

(b)

Fig. 8. Pressure of the right and left toes of the elastic strip and the displacement at the front end of the ring under the cyclic loading of 25±12.5kN

Fig. 8 also presents the exponential fitting of the total buckling pressure and the displacement at the front end of the ring in the elastic strip to the load. The relationship between the pressure and load times is as follows,

$$y = 10.343e^{-6E-06x} \tag{2}$$

Eq. (3) is the relation between the front displacement and the load at the center of the elastic strip.

$$y = 16.482e^{4E-06x} \tag{3}$$

3.3. Fatigue test results and analysis of pressure-controlled loading mode under the cyclic loading of 25± 10kN

In the processing cycle, the measurement data of 25±10 kN under the cyclic loading were taken as 2000 times. Fig. 9 shows the buckling pressure and the ring displacement curves of the elastic strip under the cyclic loading.

As shown in Fig. 9, the buckling pressure and displacement change greatly at the beginning of the test, change smoothly at the middle stage, and have large inflection points at the final stage. The elastic buckling pressure decreases from 11.22kN to 8.22 kN, less than the

prescribed minimum limit. At the beginning of the test, the ring displacement reaches 15mm because of plastic deformation, and it increases to 18.2mm at the end of the test.

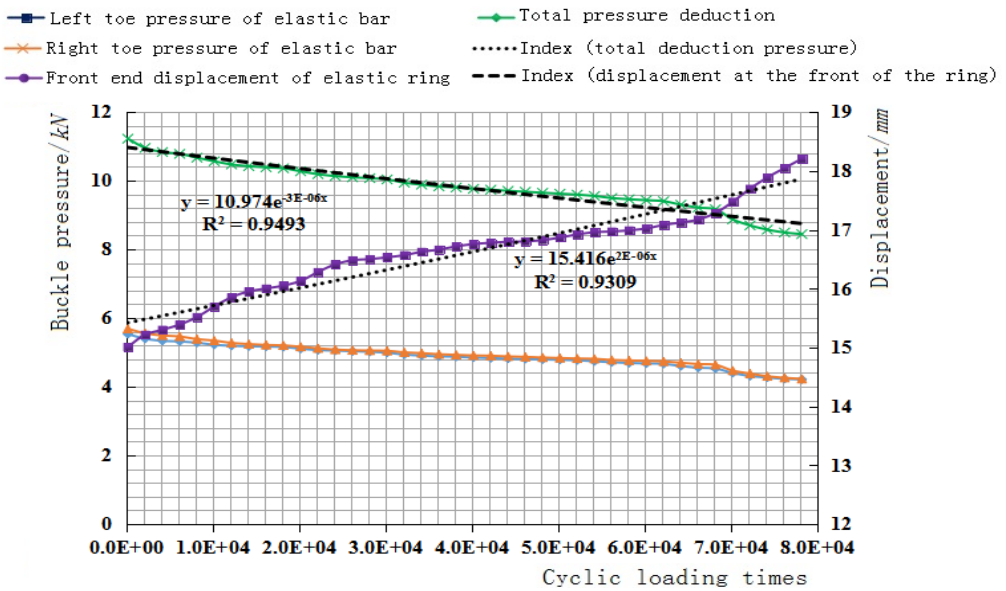

Fig. 9. Pressure of the right and left toes of the elastic strip and the displacement at the front end of the ring under the cyclic loading of 25±10kN

Fig. 9 also shows the exponential fitting of the total buckling pressure and the front end displacement of the ring in the elastic strip to the load. Eq. (4) is the relationship between the pressure and load times.

$$y = 10.974e^{-3E-06x} \tag{4}$$

Eq. (5) is the relation between the front displacement and the load at the center of the elastic strip.

$$y = 15.416e^{2E-06x} \tag{5}$$

3.4. Fatigue test results and analysis of pressure-controlled loading mode under the cyclic loading of 25± 7.5kN

The fatigue life of the elastic strip under the cyclic loading of 25±7.5 kN is close to 200,000 times. The measured data is processed with 5,000 cycle counting steps. The buckling pressure and the ring displacement curves of the elastic strip under the cyclic loading are shown in Fig. 10.

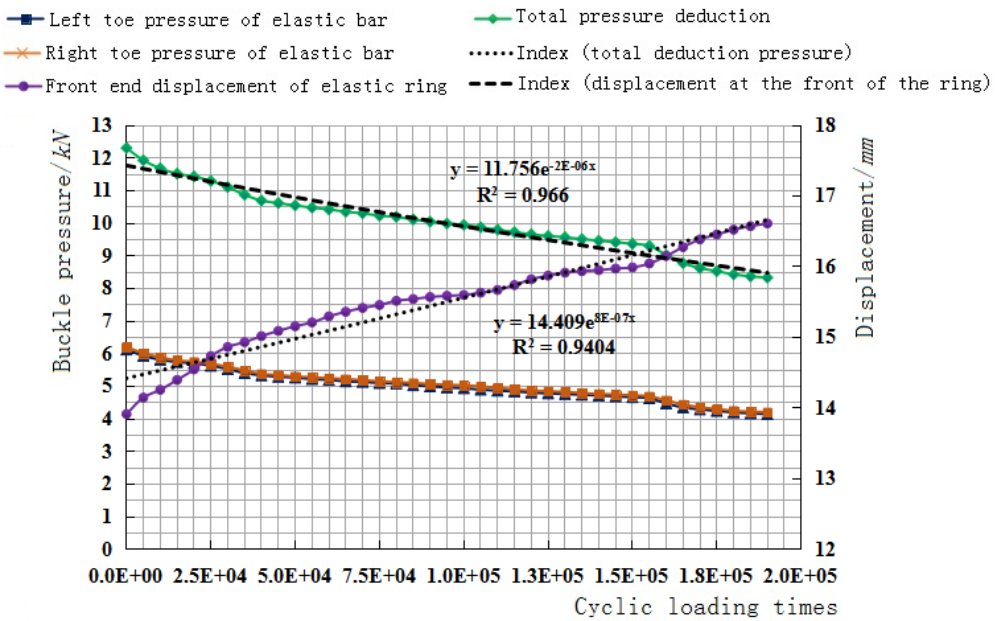

Fig.10. Pressure of the right and left toes of the elastic strip and the displacement at the front end of the ring under the cyclic loading of 25±7.5kN

As shown in Fig. 10, the buckling pressure of the elastic strip decreases from 12.29kN to 8.31kN in the initial stage, less than the specified minimum. At the beginning of the test, the displacement at the front end of the elastic strip is about 13.9mm, and that at the middle front end increases to 16.6mm at the end of the test.

Fig.10 also shows the exponential fitting of the total buckling pressure and the front end displacement of the ring in the elastic strip to the load. Eq. (6) is the relationship between the pressure and load times.

$$y = 11.756e^{-2E-06x} \tag{6}$$

Eq. (7) is the relation between the front displacement and the load at the center of the elastic strip.

$$y = 14.409e^{8E-07x} \tag{7}$$

3.5. Fatigue test results and analysis of pressure-controlled loading mode under the cyclic loading of 25±5kN

The fatigue life of the elastic strip under the cyclic loading of 25±5 kN is close to 1000,000 times. The measured data is processed with 20,000 cycle counting steps.

As shown in Table 1, the buckling pressure and the ring displacement curves of the elastic strip under the cyclic loading are shown in Fig.11.

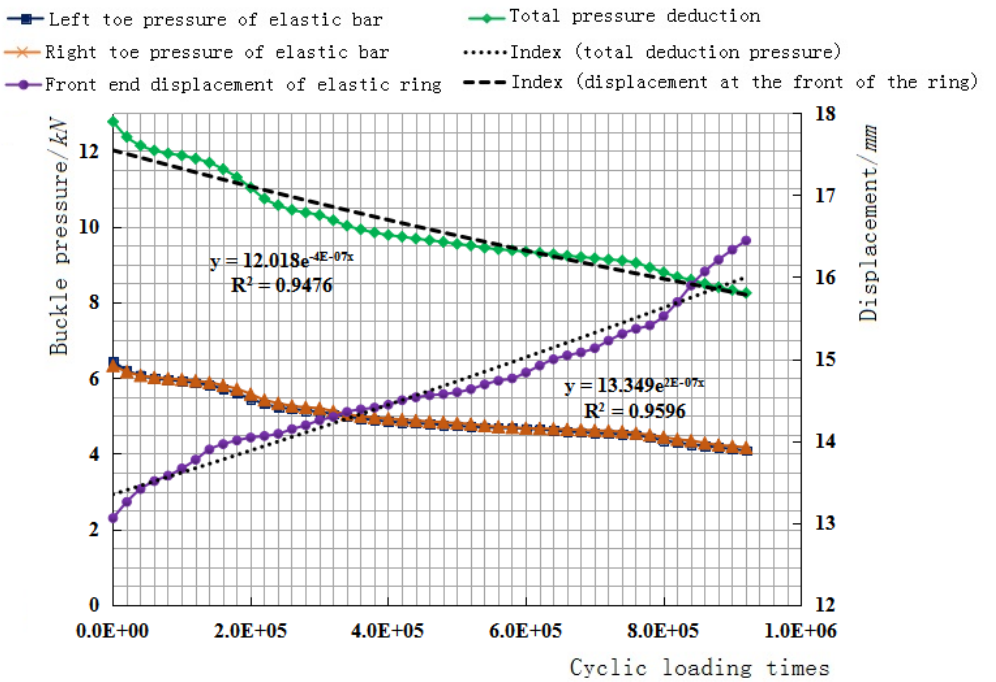

Fig.11. Pressure of the right and left toes of the elastic strip and the displacement at the front end of the ring under the cyclic loading of 25±5kN

As shown in Fig.11, due to a longer fatigue life of the elastic strip under this load, the variation of the buckling pressure and mid-front displacement of the elastic strip is larger than that under other load conditions, but the overall variation is not large. The deduction pressure decreases from 12.77kN to 8.24kN. At the beginning of the test, the displacement at the front end of the elastic strip is about 13.1mm, and that at the middle front end increases to 16.4mm in the final stage.

Fig.11 also presents the exponential fitting of the total buckling pressure and the front end displacement of the ring in the elastic strip to the loads. Eq. (8) is the relationship between the pressure and load times.

$$y = 12.018e^{-4E-07x} \tag{8}$$

Eq. (9) is the relation between the front displacement and the load at the center of the elastic strip.

$$y = 13.349e^{2E-07x} \tag{9}$$

3.6. Fatigue life curve under pressure control

When the fatigue amplitude is 25±3kN, the fatigue life is greater than 107 times. When the loading amplitude is greater than 25±5kN, the fatigue life decreases sharply, and the ratio of the decreasing amplitude of fatigue life is faster than the increasing speed of the load amplitude, as shown in Fig.12.

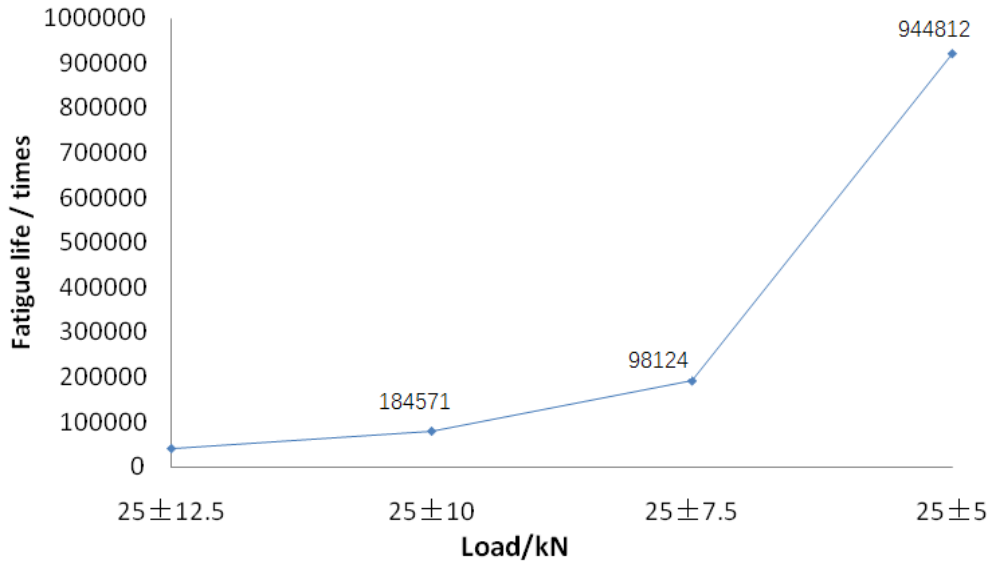

Fig. 12. Relationship between pressure-controlled loading amplitude and fatigue life

4. CONCLUSION

Elastic strip is the core component of fastener and fatigue test for elastic strips under different working conditions has good theoretical and practical significance. The pressure control method is used for fatigue tests on fastener strip. With the help of the MTS fatigue testing machine, the special mold and the corresponding sensor device, the ring displacement and the buckling pressure of the double limbs of the elastic strip are measured under the cyclic loadings of 25±5kN, 25±7.5 kN, 25±10 kN and 25±12.5 kN, respectively. Then, the fatigue test data are processed to screen out the front-end displacement of the ring and the toe-end buckling pressure of the corresponding elastic strip, taking 25 kN as the equilibrium position of the cyclic loading. According to the selected data, the displacement curves of the ring and the buckling pressure of the elastic strip are drawn under the fatigue load, and the expressions of the ring displacement and the buckling pressure of the toe and the fatigue loads are obtained. The concrete conclusions are as follows:

1) When the fatigue amplitude is 25±3 kN, the fatigue life is greater than 107 times. When the loading amplitude is greater than 25±5 kN, the fatigue life decreases sharply, and the ratio of the decreasing amplitude of fatigue life is faster than the increasing speed of the load amplitude.
2) Under the fatigue load of 25±12.5 kN and 25±10 kN, the fatigue life of the elastic strip is low. At the beginning of the test, the material has a large plastic deformation because of the excessive pressure, and the buckling pressure and the ring displacement of the elastic strip change greatly. Then the buckling pressure continues to decrease, and the front displacement of the ring in the elastic strip increases continuously. In the final stage, the buckling pressure of the elastic strip is less than the minimum value of the specification, and the ring displacement is close to the upper limit of the range, indicating that the elastic strip is completely invalid. Under the cyclic loading of 25±7.5 kN and 25±5 kN, the fatigue

life of the elastic strip is obviously improved. From the beginning to the final stage of the test, the pressure and shift of the ring are relatively stable. In the final stage, the deduction pressure is still larger than that specified in 9 kN, and the ring displacement is also less than the upper limit of the elastic range.

3) In the fatigue test, the attenuation of the buckling pressure at the toe of the elastic strip is 22%-33%, and the displacement at the front end of the ring increases by 18%-25%. The buckling pressure at the toe end and the displacement curve at the front end of the ring have the characteristics of "increasing step-by-step" and "decreasing step-by-step" because of the periodic plastic deformation under the cyclic loading. When the plastic deformation is large, the buckling pressure and displacement change greatly, while the buckling pressure and displacement change little when there is small or no plastic deformation.
4) According to the results, the buckling pressure curve and the displacement curves of the ring in the elastic strip are drawn. The equations of the bucking pressure curves and the ring displacement are fitted to estimate the service performance of the elastic strip.

ACKNOWLEDGEMENTS

The authors acknowledge the National Natural Science Foundation of China (Grant: 51868033).

REFERENCES

[1] Valikhani, M, Younesian, D., Application of an optimal wavelet transformation for rail-fastening system identification in different preloads. Measurement, 2016, 82: p. 161-175.

[2] Jin, X.S., Wu, Y., Liang, S.L., Wen, Z.F., Mechanisms and Countermeasures of Out-of-Roundness Wear on Railway Vehicle Wheels. Journal of Southwest Jiaotong University, 2018, 53(1):p. 1-14.

[3] Xiao, J.L., Liu, H., Liu, G.Z., Wang, Y., Wang, P., Study on Characteristics and Law of Longitudinal Resistance Hysteretic Curves of Ballast Bed of High. Journal of the China Railway Society, 2018, 40(2): p. 91-99.

[4] Xu, L., Zhai W.M., Stochastic Model Used for Temporal-spatial Analysis of Vehicle-track Coupled Systems. Journal of the China Railway Society, 2018, 40(1): p. 74-79.

[5] Feng, Q.S., Lei, X.Y., Lian, S.L., A dynamic model of ground for high-speed railway with track random irregularities. Journal of Vibration Engineering, 2013, 26(6): p. 927-934.

[6] Bae, H.U., Park, S.J., Yun, K.M., Park, B.H., Lim, N.H., Statistical Characteristics for Longitudinal Friction Behavior of Rail Fastening System for Concrete Track. Journal of Korea Academia-Industrial cooperation Society, 2015, 16(11): p. 7870-7877.

[7] Zhao, G.T., Method for Determining the Rigidity of Railway Track. China Railway Science, 2005, (1): p. 1-5.

[8] Wang, P., Zhou, C.S., Wei, K., Xu, H., The Energy Research on the Wheel- rail System in the Process of Stochastic Vibration. Journal of Railway Engineering Society, 2015, 32(5): p. 30-34+41.

[9] Zhao, C.Y., Wang, P., Zhu, Y., Zhao, W.H., Xiao, J.L., Theoretical analysis and test for vibration damping fastenings. Journal of Vibration and Shock, 2012, 31(23): p. 191-196.

[10] Cox, S., Installation and testing of vibration reducing track fastenings within the CONVURT project. Proceedings of the Tenth International Congress on Sound and Vibration. Stockholm: Institute of Acoustics, 2003, p. 379-386.

[11] Bösterling, W., Innovative elastic rail fastening systems for slab track. ZEV Rail Glasers Annalen, 2011, 135(5): p. 172-175.

[12] Krüger, F., New continuous rail fastener systems to reduce vibrations-investigations on a test rig and calculations by FEM. ZEV UND DET GLASERS ANNALEN, 2000, 124(5): p. 327-336.

[13] Liu, X.Y., Zhang, Z.W., Wan, Z.B., Influence of fastener stiffness mutation in ballastless track on dynamic characteristics of high-speed trains. Journal of Railway Engineering Society, 2014, 31(9): p. 53-58.

[14] Ren, J.J., Zhao. H.W., Li, X., Xu, K., Analysis of Harmonic Response of CRTS III Prefabricated Slab Track with Anti-vibration Structure. Journal of Railway Engineering Society, 2016, 33(3): p. 44-50.

[15] Zhao, P.R., Xiao, J.L., Liu, X.Y., The Influence of the Displacement at Bridge Ends to the Fastening Systems Used on Ballastless Tracks. Journal of the China Railway Society, 2008, (5): p. 68-73.

[16] Wei, Y.H., Xu, H.S., Niu, B., Laboratory test and numerical analysis on the mechanical behaviors of the slab track fastener due to the beam-ending deformation. China Railway Science, 2010, 31(6): p. 43-49.

[17] Wei, K., Zhang, P., Dou, Y.L., Wang, P., Zhou, C.S., Experimental Study on Temperature-dependent Mechanical Property of Rail Pads Used in Non-ballasted Track of High-speed Railway. Journal of the China Railway Society, 2016, 38(7): p. 98-104.

[18] Kimmo, H., Stress calculations for direct fastening track. Rail International, 2001, 32(1): p. 35-43.

[19] Casado, J.A., Carrascal, I., Diego, S., Polanco, J.A., Gutiérrez-Solana, F., García, A., Mechanical behavior of recycled reinforced polyamide railway fasteners. Polymer Composites, 2010, 31(7):p. 1142-1149.

[20] Diego, S., Casado, J. A., Carrascal, I., Polanco, J. A., & Gutiérrez-Solana, F., Experimental validation of an adjustable railway fastening for slab track. Journal of Testing and Evaluation, 2010, 38(5):p. 598-608.

[21] Koh, T., Shin, M., Bae, Y., Hwang, S., Structural performances of an eco-friendly prestressed concrete sleeper. Construction and Building Materials, 2016, 102(Part 1): p. 445-454.

[22] Zhu, J.Y., On the effect of rail fastener support failure on the dynamic behavior of railway track. Journal of Vibration Engineering, 2011, 24(2): p. 158-163.

[23] Wu, Z., Ma, W., Xiao, H. X., Zhang, J. K., Study on fatigue life of ballastless track fastener springs based on a fatigue test. International Journal of Structural Integrity, 2020, 11(6): p. 737-750.

[24] Zakeri, J. A., Xia, H., & Fan, J. J., Effects of unsupported sleeper on dynamic responses of railway track. Journal of Northern Jiaotong University, 2000, (1):p. 50-55.

[25] Xiao, X.B., Wen, Z.F., Jin, X.S., Effect of Track Support Failure on Dynamic Responses and Riding Comfort of Vehicle System. Journal of the China Railway Society, 2007, (6): p. 26-33.

[26] Zhou, L., Shen, Z.Y., Dynamic analysis of a high-speed train operating on a curved track with failed fasteners. Journal of Zhejiang University SCIENCE A, 2013, 14: p. 447-458.

[27] Tian, C.X., Yan, H., Xiong, W., Discussion on the Space between Fastenings on High-speed Railway. Railway Standard Design, 2013, (8): p. 32-36.

[28] Zhu, S.Y., Cai, C.B., Yin, B., Xu, P., Dynamic analysis of rail fastening clip in high-speed railway. Engineering Mechanics, 2013, 30(6): p. 254-258+287.

[29] Wang, S.W., Analysis of Structural Damping Property of Rail Fastening Rubber Absorber. Railway standard design, 2015, 59(1): p. 37-41+46.

[30] Sun, L., Duan, Y.F., Yang X., Static Response Analysis of CRTS III Ballastless Track Structure. Journal of Railway Engineering Society, 2013, (11): p. 32-39.

[31] Zhang, S.F., Analysis on fastening force of ballastless track. Chengdu: Southwest Jiaotong University. 2016

[32] Rakow, A, Chang, F.K., A structural health monitoring fastener for tracking fatigue crack growth in bolted metallic joints. Structural Health Monitoring, 2012, 11(3): p. 253-267.

[33] Du, Y.L., Zhang, Y.Z., Zhao, W.G., Construction of safety monitoring system for high-speed railway line engineering. China Civil Engineering Journal, 2012, 45(S2): p. 59-63.

[34] Du, Y.L., Su, M.B., Liu, Y.H., Wang, Q.M., Study on the Long-term Health Monitoring and Safety Evaluation System for the Wuhan Yangtze River Bridge. Journal of the China Railway Society, 2015, 37(4): p. 101-110.

[35] Xiong, J.Y., Shen, Z.Y., Rise and future development of Chinese high-speed railway. Journal of Traffic and Transportation Engineering, 2021, 21(5):p. 6-29.